Journal of Alloys and Compounds 508 (2010) 406–411

Contents lists available at ScienceDirect

Journal of Alloys and Compounds

journal homepage: www.elsevier.com/locate/jallcom

# Electrical conductivity and dielectric spectroscopic studies of PVA–Ag nanocomposite films

Suman Mahendia[a,*], A.K. Tomar[a,b], Shyam Kumar[a]

[a] Department of Physics, Kurukshetra University, Kurukshetra 136119, India
[b] Department of Physics, Kurukshetra Institute of Technology and Management, Kurukshetra 136119, India

ARTICLE INFO

*Article history:*
Received 15 March 2010
Received in revised form 2 August 2010
Accepted 18 August 2010
Available online 27 August 2010

*Keywords:*
Silver nanoparticles
SPR
Dielectric constant
dc Conductivity
ac Conductivity
Electric modulus
Relaxation time

ABSTRACT

Poly(vinyl alcohol)–silver (PVA–Ag) nanocomposite films were prepared by the soft chemical route. Effect of concentration of embedded Ag nanoparticles on conductivity and dielectric relaxation behaviour of these nanocomposite films has been studied. An increase in dc conductivity from $1.38 \times 10^{-11}$ to $9.17 \times 10^{-11}$ S/cm and decrease in frequency dependent dielectric constant (from 1.74 to 1.07 at 75 kHz) are observed with the increase in concentration of Ag nanoparticles in PVA from 0 to 1.32 wt%. The values of ac conductivity and polarization relaxation time, deduced from dielectric data, also corroborate towards the enhanced conducting behaviour of PVA matrix with increase in the concentration of embedded Ag nanoparticles.



## 1. Introduction

Metal nanoparticles based nanocomposites are now one of the main focus points of research because of their technological applications including the conceptual understanding of involved physics and chemistry [1–5]. It is well established that polymers, as dielectric materials, are excellent host matrices for encapsulation of metal nanoparticles like silver, gold, etc., as they act both as reducing as well as capping agents and also provide environmental and chemical stability [6,7]. The obtained nanocomposites might exhibit improved optical, electrical, thermal and mechanical properties [8,9]. Many reports in literature show attempts for synthesis of metal nanoparticles based polymer nanocomposites, with the possibility of variation in their optical and electrical properties for their application in high performance capacitors, conductive inks and other electronic components [10,11]. For their application in opto-electronic, electrical and optical devices, biomedical science, sensors, etc., main key points are selection of polymer–metal nanoparticles combination, controlling the particles size, their concentration and distribution within the polymer matrix [12–14]. Further, detailed investigation of concentration dependent dielectric loss and polarization effects of polymers deserves special importance in dielectric based opto-electronic and electrical devices [9,15,16].

We have selected poly(vinyl alcohol) (PVA) polymer as the host matrix in the present work due to the advantage of its high mechanical strength, water-solubility, good environmental stability, easy processability, moderate and dopant dependent electrical conductivity along with its consideration among the best polymers as host matrix for silver nanoparticles [17–19].

In this communication, we focus on dielectric relaxation and electrical conductivity behaviour of PVA–Ag nanocomposite films at room temperature with varying concentration of chemically prepared silver nanoparticles.

## 2. Experimental

Hydrosol of silver nanoparticles has been chemically synthesised by chemical reduction of silver nitrate through sodium borohydride [20]. For this, aqueous solution of silver nitrate is added drop wise to cooled sodium borohydride solution under continuous stirring. After that, few drops of 0.3% PVP were added as stabilizing agent. PVA–Ag nanocomposites with varying concentration of silver nanoparticles have been prepared by mixing different quantities of silver hydrosol to PVA solution. To make films, the prepared composite solutions were casted to plastic Petri-dishes and after evaporation of the solvent at ambient temperature, films were peeled off. The thickness of the films was measured using digital micrometer screw gauge, with least count of 1 μm and found to be ~50 μm. In order to determine the content of the Ag nanoparticles by weight, these films were subjected to Atomic Absorption Spectroscopy (AAS). The measured concentration of Ag in these films has been tabulated in Table 1.

* Corresponding author. Tel.: +91 9466095387.
*E-mail address:* mahendia@gmail.com (S. Mahendia).

0925-8388/$ – see front matter © 2010 Elsevier B.V. All rights reserved.
doi:10.1016/j.jallcom.2010.08.075

**Table 1**
The value of dc conductivity and relaxation time for PVA–Ag nanocomposites with varying concentration of Ag nanoparticles embedded in it.

| Sample | dc Conductivity ($\sigma_{dc}$) ($\times 10^{-11}$ S/cm) | Relaxation time ($\tau_p$) ($\times 10^{-7}$ s) |
|---|---|---|
| Pure PVA | 1.38 | – |
| PVA + 0.13 wt% Ag | 2.03 | – |
| PVA + 0.26 wt% Ag | 2.99 | 22.49 |
| PVA + 0.41 wt% Ag | 4.23 | 19.66 |
| PVA + 0.50 wt% Ag | 4.84 | 14.93 |
| PVA + 0.80 wt% Ag | 8.80 | 7.75 |
| PVA + 1.32 wt% Ag | 9.17 | 5.74 |

### 2.1. UV–visible spectroscopy

To check the formation of Ag nanoparticles within a hydrosol and estimate their size, UV–visible absorption spectrum was recorded using Shimandzu Double Beam Double monochromator UV–Visible Spectrophotometer (UV–Visible 2550) in the wavelength range of 190–900 nm with the resolution of 0.5 nm. The absorption spectrum of Ag hydrosol was recorded by taking distilled water as reference at room temperature using 1 cm quartz cuvette.

### 2.2. Transmission electron microscopy (TEM)

For determination of the size of as-prepared silver nanoparticles and their distribution, TEM measurements were carried out using Hitachi "H-7500" TEM operated at 120 kV. To record the TEM images, few drops of hydrosol were dropped onto carbon coated gold grid while for nanocomposite samples, small part of the respective films were cut and redissolved in double distilled water and then dropped on to the grid.

### 2.3. Electrical measurements

The *I–V* characteristics were studied with Keithley 5110 Digital Electrometer using 8009 Resistivity Text Fixture with computer interface by the two probe method at room temperature. The measurements were carried out by measuring the current ($I$) on application of voltage ($V$) in the range 0–100 V in multiple steps of 5 V. The dc conductivity was calculated using the relation

$$\sigma_{dc} = \frac{d}{RA}\,(\mathrm{S/cm})$$

where $d$ is the sample thickness, $A$ is the area of electrode and $R$ is the resistance offered by the sample, which is estimated from the *I–V* data.

### 2.4. Dielectric measurements

To study the frequency dependent dielectric properties, Aligent 4285A Precision LCR meter was used. The capacitance ($C$) and dielectric loss ($\varepsilon''$) were recorded at room temperature for the frequency range 75 kHz to 5 MHz. Using the capacitance values $C$, the dielectric constant ($\varepsilon'$) (component of energy stored in each cycle of the electric field) can be calculated using the relation

$$\varepsilon' = \frac{Cd}{\varepsilon_0 A}$$

where $d$ is the thickness of the sample, $A$ is the area of the electrode and $\varepsilon_0$ is the permittivity of the free space. The frequency dependent variation in ac conductivity $\sigma_{ac}$ (component of energy loss) and electric modulus ($M$) can also be studied from the dielectric data using the following relations [15,17,18]

$$\sigma_{ac} = 2\pi f \varepsilon_0 \varepsilon''$$

$$M = \frac{1}{\varepsilon^*(=\varepsilon' + i\varepsilon'')} = M' + iM''$$

where $M' = \varepsilon'/(\varepsilon'^2 + \varepsilon''^2)$; real part and $M'' = \varepsilon''/(\varepsilon'^2 + \varepsilon''^2)$; imaginary part.

The main advantage of calculating $M'$ is to suppress electrode effect. Further, from the imaginary part of electrical modulus ($M''$), the relaxation time ($\tau_p$) of the orientation of dipoles can be obtained using the relation [18]

$$\tau_p = \frac{1}{\omega_p}$$

where $\omega_p$ is the angular frequency corresponding to the peak of $M''$ versus log frequency curves.

## 3. Results and discussion

### 3.1. Ag nanoparticles

Fig. 1 presents the UV–visible absorption spectrum of Ag hydrosol synthesized by chemical reduction method, as discussed above. The spectrum clearly shows an intense absorption band peaking at ~400 nm, showing the characteristic Surface Plasmon Resonance (SPR) band of silver nanoparticles [3,13]. Further, almost symmetric shape and narrow FWHM of SPR band indicate that the synthesized silver nanoparticles are nearly spherical in shape [8]. From the FWHM ($\Delta E_{1/2}$) of SPR band, the diameter ($d$) of silver nanoparticles has been estimated by assuming free particles behaviour of conduction electron [21], using the relation [13]

$$d = \frac{2h\nu_f}{\Delta E_{1/2}}$$

where $\nu_f$ ($1.39 \times 10^6$ m/s) is the Fermi velocity of electrons in bulk silver and $h$ is the Planck's constant. The average diameter of Ag nanoparticles has been found to be of the order of 11 nm. The shape and size of silver nanoparticles have also been analyzed through TEM images (Fig. 2). These images clearly indicate the spherical shape of Ag nanoparticles with their average diameter ~11 ± 3 nm, in agreement with the results of SPR prediction.

### 3.2. PVA–Ag nanocomposite films

#### 3.2.1. TEM study

To check the distribution of Ag nanoparticles with their varying concentrations within the PVA matrix, the TEM photographs were taken and shown in Fig. 3. It is clearly observable from this figure that the Ag nanoparticles are not agglomerated, except slightly at 1.32 wt% concentration, and are well distributed within the polymer matrix. The non-agglomeration may be due to the formation of sterric coils of PVP chains around the Ag nanoparticles, which was added during their synthesis. This provides chemical stability to nanoparticles [7] even after being embedded in PVA matrix.

#### 3.2.2. dc Conductivity

The variation in dc electrical conductivity of these samples with different Ag nanoparticles concentration (0.13, 0.26, 0.41, 0.50, 0.80 and 1.32 wt%) is shown in Fig. 4 and the corresponding values are tabulated in Table 1. From this figure and table, it is clear that the conductivity of PVA is increased by ~1 order on doping it with

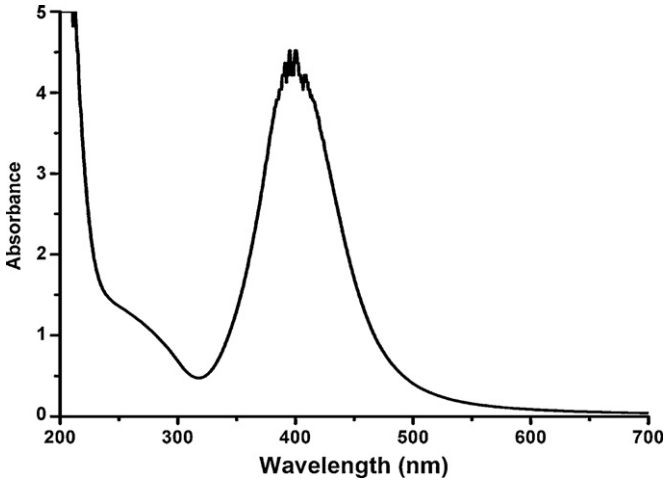


**Fig. 1.** UV–visible spectrum of chemically prepared hydrosol of Ag nanoparticles.

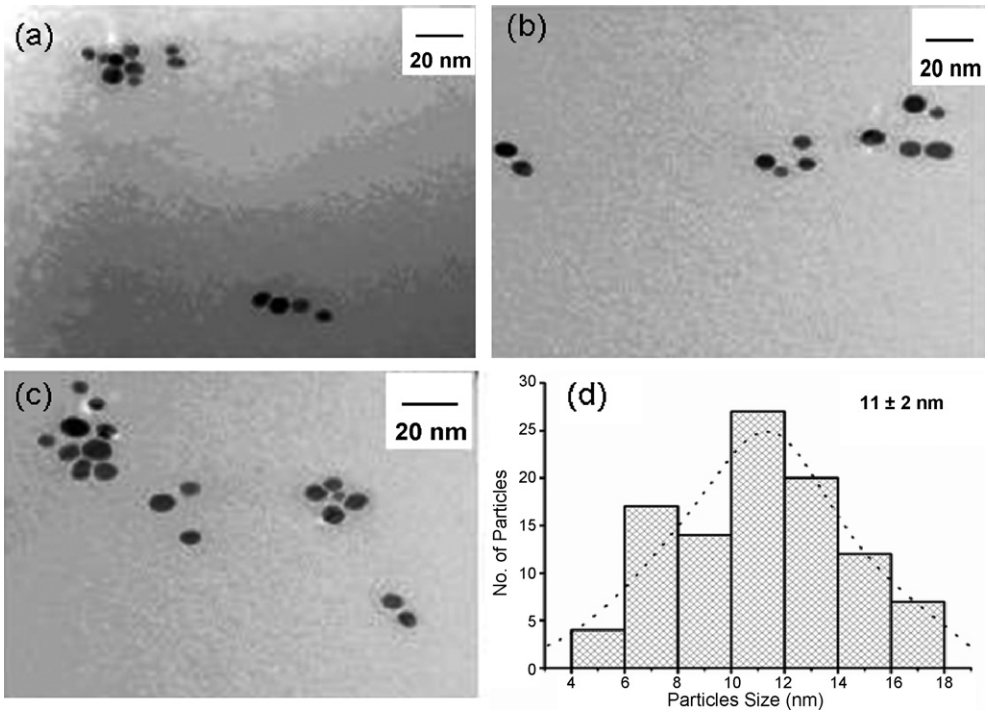


**Fig. 2.** TEM images of chemically prepared hydrosol of Ag nanoparticles and their size distribution.

1.32 wt% of Ag nanoparticles. This can be explained on the basis of the formation of charge transfer complexes (CTCs) inside the polymer chain network after embedding of Ag nanoparticles as dopant. It is known that in semi-crystalline polymers, the dopant forms CTCs and hence reduces barrier height between the trapping sites, which in turn provides a conducting path through the amorphous regions of the polymer matrix resulting in enhanced conductivity [17]. Such phenomena are supposed to decrease the

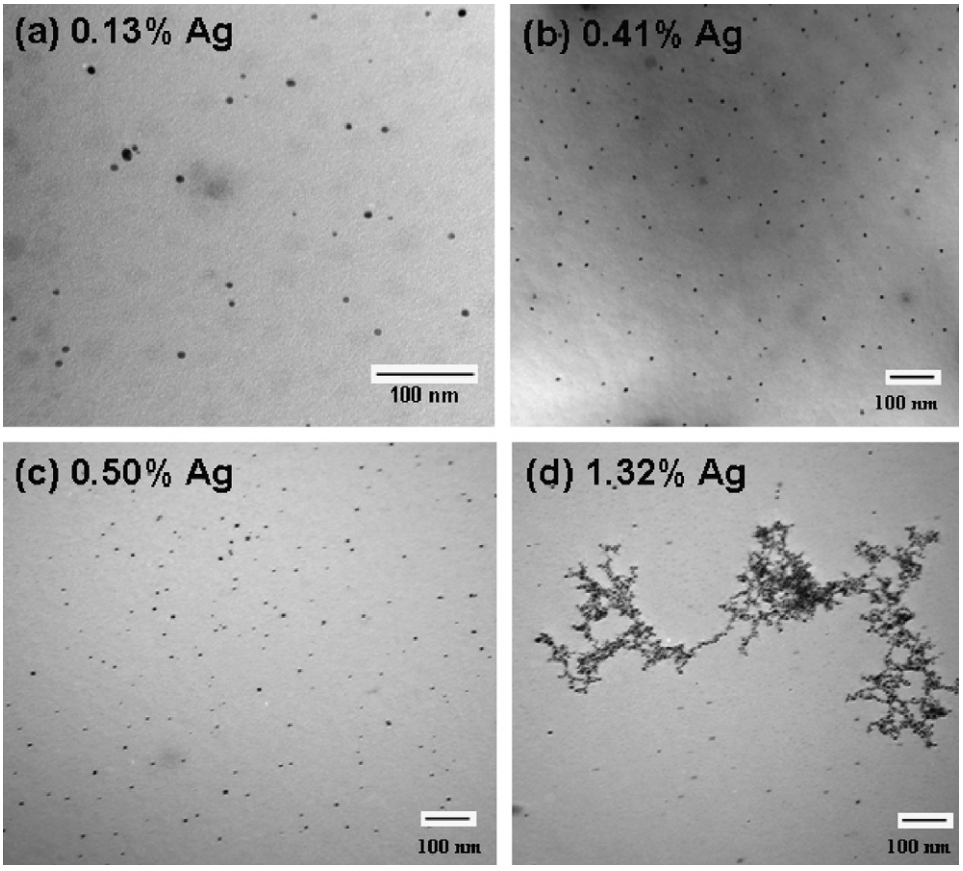


**Fig. 3.** TEM images for PVA–Ag nanocomposites with different concentration (wt%) of Ag nanoparticles.

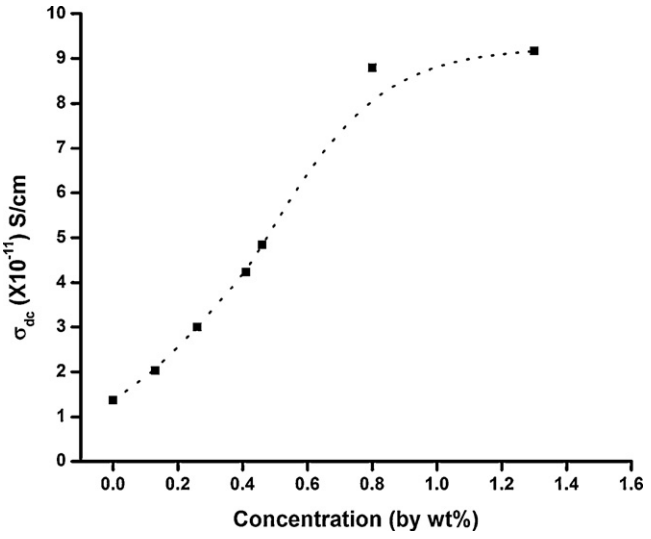


**Fig. 4.** Variation in dc conductivity ($\sigma_{dc}$) of PVA–Ag nanocomposites with concentration (wt%) of Ag nanoparticles.

activation energy of the carrier and increase the mobility towards the electrode during polarization. Accordingly, in the present case, it is reasonable to assume that Ag nanoparticles fill the free volume holes (amorphous phase) and occupy the interstitial positions between the polymer chains in amorphous phase and link these chains to some kind of bonds by charge exchange process between the nanoparticles as dopant and PVA chain network. Further, this complex formation increases with doping level. As a result, both charge carrier density and the PVA conductivity are increased. These CTCs cause reduction of the crystalline–amorphous interface which further decrease the interfacial barrier and, thus, increase the transition probability of electron hopping across the barrier and insulator chains. Such hopping process can also be explained on the basis of the percolation theory suggesting that the Ag nanoparticles may act as conductive fillers in the polymer matrix, which provide the continuous conductive pathways for the transfer of charge from one CTC to another [22,23].

### 3.2.3. Dielectric studies

Fig. 5(a) and (b) shows the variation in dielectric constant $\varepsilon'$ and dielectric loss $\varepsilon''$, respectively with frequency at temperature 307 K. As shown in Fig. 5(a), a decrease in the value of $\varepsilon'$ with the increase in frequency has been observed. It can be seen that for pure PVA, the value of $\varepsilon'$ is ~1.74 at frequency 75 kHz, which gradually decreases to ~1.02 at 5 MHz [16,24,25]. Similar behaviour is also observed in a number of other polymers like PVP, PMMA, etc., verifying the fact that for polar materials, the value of $\varepsilon'$ is high for low frequency range and begins to drop as frequency increases [26–28]. This can be appropriately explained on the basis of the electrode effect and interfacial effect of the sample, i.e., charge carriers being blocked at the electrodes. This may be attributed to the tendency of dipoles in polymeric samples to orient themselves in the direction of applied field in the low frequency range. On the other hand, due to polarization effects and smaller tendency of dipoles to orient themselves according to the field variation at high frequencies, value of dielectric constant decreases [29]. As also depicted from this figure, the value of $\varepsilon'$ decreases as the concentration of the embedded Ag nanoparticles increases, which directs towards the reduction in insulating characteristic behaviour of PVA after doping, and thus, convincing the dc conductivity results of enhanced conducting nature after the embedding of Ag nanoparticles in PVA.

The variation of dielectric loss ($\varepsilon''$) with frequency for PVA–Ag nanocomposite films at different concentration of Ag nanoparticles is shown in Fig. 5(b). It is clear from this graph that dielectric loss decreases with an increase in frequency. The larger value of the loss factor or dielectric loss at low frequency could be due to the mobile charges within the polymer matrix. At high frequency, periodic field reversal is so fast that there is no excess ion diffusion in the direction of electric field [26,27]. Polarization due to charge accumulation decreases, leading to the decrease in the value of loss factor. Furthermore, high value of dielectric loss for higher concentration of embedded Ag nanoparticles can be understood in terms of electrical conductivity, which is associated with the dielectric loss and shown in Fig. 6. It is clearly observable from this figure that ac conductivity increases as the dopant concentration increases. In PVA, as the bond rotates with frequency, the existing flexible polar groups with polar bonds cause dielectric α-transition. Thus, there is a change in chemical composition of the polymer repeated unit due to the formation of CTCs within the PVA chains, which in turn makes the polymer chains more flexible and hence enhances both the dc and ac electrical conductivity [17,18].

Fig. 7(a) and (b) shows the calculated values of real and imaginary parts of electrical modulus for the nanocomposite films for

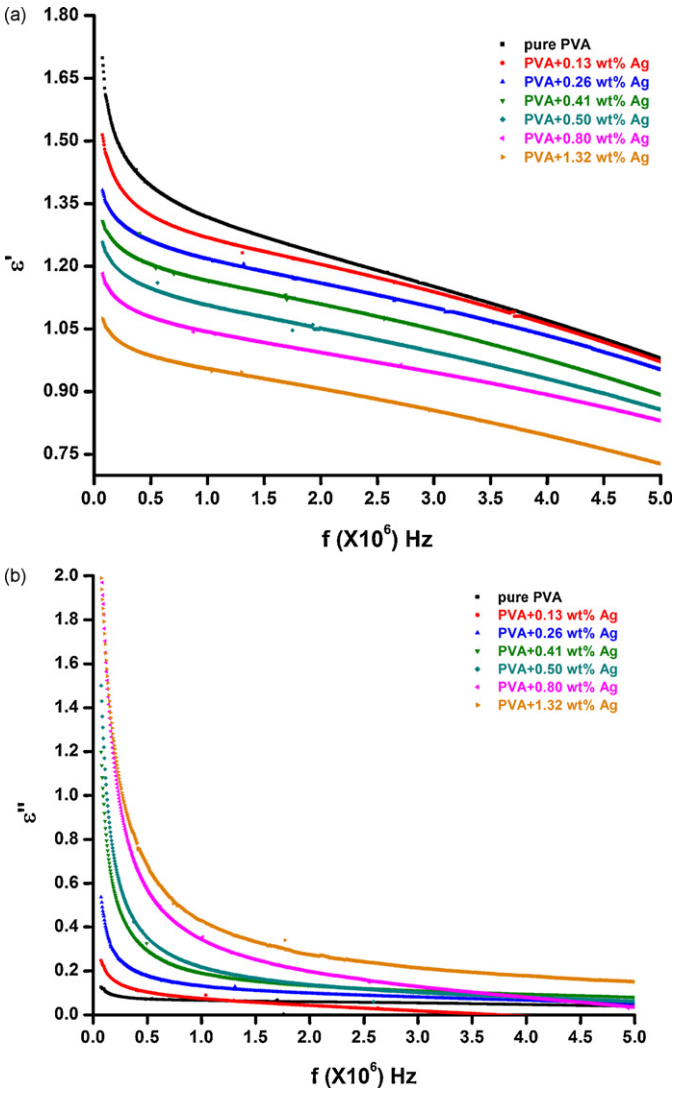


**Fig. 5.** (a) Variation in dielectric constant ($\varepsilon'$) with frequency for different concentration (wt%) of Ag nanoparticles in PVA. (b) Variation in dielectric loss factor ($\varepsilon''$) with frequency for different concentration (wt%) of Ag nanoparticles in PVA.

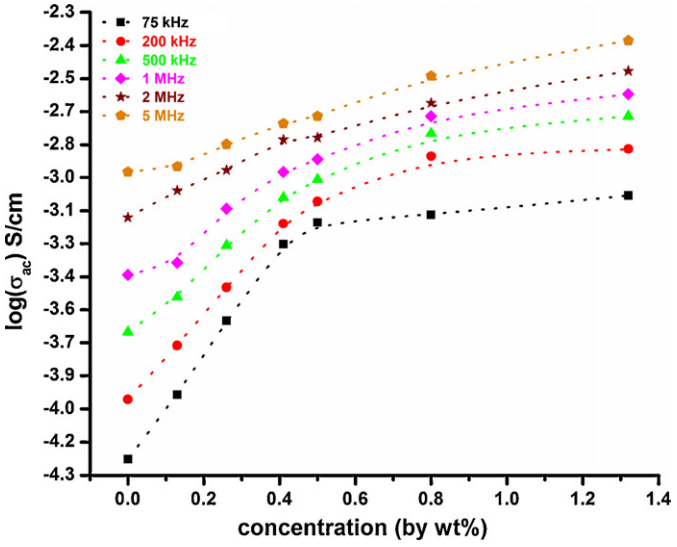


**Fig. 6.** Variation in ac conductivity ($\sigma_{ac}$) of PVA–Ag nanocomposites with concentration (wt%) of Ag nanoparticles for different frequencies.

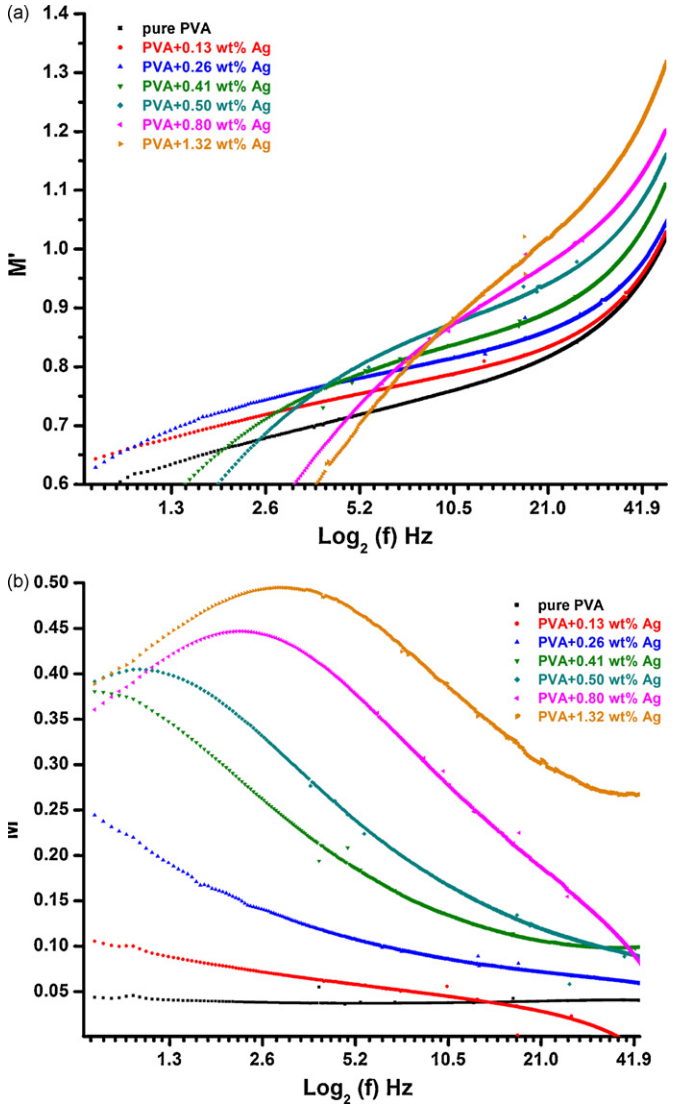


**Fig. 7.** (a) Variation in real part of electric modulus ($M'$) with frequency for different concentration (wt%) of Ag nanoparticles in PVA. (b) Variation in imaginary part of electric modulus ($M''$) with frequency for different concentration (wt%) of Ag nanoparticles in PVA.

different dopant concentration of Ag nanoparticles. The low value of $M'$ indicates the removal of electrode polarization [15–18]. The spectrum of $M''$ shows an asymmetric peak approximately centred in the dispersion region of $M'$ which corresponds to the relaxation frequency. The peak appears to shift towards higher frequency as the dopant concentration increases. Table 1 shows the relaxation time ($\tau_p$) for the different samples. From the whole data, it can be concluded that with the increasing concentration of Ag nanoparticles as dopant, the relaxation time for dipole orientation reduces, which confirms the explanation of the dielectric constant and loss factor characteristics with increase in dopant concentration, which also contributes towards the enhanced conductivity of PVA–Ag nanocomposites.

## 4. Conclusions

The PVA–Ag nanocomposite films with varying concentration of Ag nanoparticles were synthesized chemically through ex situ route. It has been observed that the concentration of silver nanoparticles has greatly influenced the electrical conductivity and dielectric properties of PVA matrix. Increase up to 1 order of conductivity while gradual decrease in dielectric constant has been observed with increasing concentration of embedded nanoparticles in PVA with maximum up to 1.32 wt% of Ag. Further, these nanocomposite films exhibit a combination of electronic polarization of PVA matrix and intrinsic dielectric anisotropy due to the formation of CTCs through embedding of Ag nanoparticles. Relaxation time becomes shorter (0.57 μs) with increase in concentration of Ag nanoparticles (up to 1.32 wt %), clearly indicating the relaxation of dipoles through multiple paths due to increased availability of free charge carriers as CTCs.

## Acknowledgement

The authors are highly thankful to Dr. Ravi Kumar and his students (IUAC, New Delhi, India) for their kind help in providing the facility for dielectric measurements.

## References

[1] A. Balamurugan, K.-C. Ho, S.-M. Chen, Synth. Met. 159 (2009) 2544–2549.
[2] R.A. de Barros, C.R. Martins, W.M. de Azevedo, Synth. Met. 155 (2005) 35–38.
[3] A. Heilman, Polymer Films with Embedded Metal Nanoparticles, Springer-Verlag, Berlin, Heidelberg, 2003.
[4] P.H.C. Camargo, K.G. Satyanarayana, F. Wypych, Mater. Res. 12 (2009) 1–39.
[5] B. Raneesh, A. Pragatheeswaran, P. Dhanasekaran, P. Chandrasekaran, N. Kalarikkal, J. Ovonic Res. 6 (2010) 187–191.
[6] N. Singh, P.K. Khanna, Mater. Chem. Phys. 104 (2007) 367–372.
[7] P.K. Khanna, R. Gokhale, V.V.V.S. Subbarao, A.K. Vishwanath, B.K. Das, C.V.V. Satyanarayana, Mater. Chem. Phys. 92 (2005) 229–233.
[8] V.V. Vodnik, J.V. Vukuvic, J.M. Nedeljkovic, Colloid Polym. Sci. 287 (2009) 847–851.
[9] A. Gautam, S. Ram, Phys. Status Solidi A 206 (2009) 1471–1477.
[10] O.L.A. Monti, J.T. Fourkas, D.J. Nesbitt, J. Phys. Chem. B 108 (2004) 1604–1612.
[11] K.L. Kelly, E. do Coronado, L.L. Zhao, G.C. Schatz, J. Phys. Chem. B 107 (2003) 668–677.
[12] H. Weickmann, J.C. Tiller, R. Thomann, R. Mulhaupt, Macromol. Mater. Eng. 290 (2005) 875–883.
[13] U. Keirbeg, M. Vollmer, Optical Properties of Metal Clusters, Springer Series in Material Science, vol. 25, Springer-Verlag, Berlin, 1995.
[14] S. Chen, J.M. Sommers, J. Phys. Chem. B 105 (2001) 8816–8820.
[15] P. Dutta, S. Biswas, S. Kumar de, Mater. Res. Bull. 37 (2002) 193–200.
[16] Ch.V.S. Reddy, X. Han, Q.-Y. Zhu, L.-Q. Mai, W. Chen, Microelecon. Eng. 83 (2006) 281–285.
[17] R.F. Bhajanti, V. Ravindrachary, A. Harisha, G. Ranganathaiah, G.N. Kumaraswamy, Appl. Phys. A 87 (2007) 797–805.
[18] M.H. Harun, E. Saion, A. Kassim, E. Mahmud, M.Y. Hussain, I.S. Mustafa, J. Adv. Sci. Arts 1 (2009) 9–16.
[19] E. Tuncer, I. Sauers, D.R. James, A.R. Ellis, M.P. Paranthaman, A. Goyal, K.L. More, Nanotechnology 18 (2007), 325704 (5pp.).
[20] S.D. Solomon, M. Bahadory, A.V. Jeyarasingam, S.A. Ruthkowsky, C. Boritz, L. Mulfinger, J. Chem. Edu. 84 (2007) 322–325.

[21] G.W. Arnold, J. Appl. Phys. 46 (1975) 4466–4473.
[22] C.U. Devi, A.K. Sharma, V.V.R.N. Rao, Mater. Lett. 56 (2002) 167–174.
[23] A. Kiesow, J.E. Morris, C. Radehaus, A. Heillman, J. Appl. Phys. 94 (2003) 6988–6990.
[24] J.A. Cambell, A.A. Goodwin, G.P. Simon, Polymer 42 (2001) 4731–4741.
[25] S. Abd El Mongy, Aus. J. Basic Appl. Sci. 3 (2009) 1954–1963.
[26] P.B. Bhargav, B.A. Sarada, A.K. Sharma, V.V.R.N. Rao, J. Macromol. Sci. Part A: Pure Appl. Chem. 47 (2010) 131–137.
[27] D. Mardare, G.I. Rusu, J. Optoelectron. Adv. Mater. 6 (2004) 333–336.
[28] T. Fuyuki, H. Matsunmi, Jpn. J. Appl. Phys. 25 (1986) 1288–1291.
[29] C.S. Ramya, T. Savutha, S. Selvasekarapandian, G. Hirankumar, Ionics 11 (2005) 436–441.